

Multi-Infill Strategies for Optimizing Tensile Properties in FDM-Printed PLA+ Components

Noor Faraz Khan*, Dr. Abdul Shakoor*, Muhammad Bilal Afzal**, Atif Shehzad***, Fazli Subhan**,
Kamran Ahmad****

*Mechanical Engineering, University of Engineering & Technology Peshawar

**Pakistan Council of Scientific & Industrial Research

***NED University of Engineering & Technology

****Sui Northern Gas Pipelines Limited

Abstract- The rapid advancements in Additive Manufacturing (AM) technologies have revolutionized modern production methods, providing unparalleled opportunities for sustainable innovation in the process industry. This study focuses on the tensile investigation of multi-infill lattice structure components fabricated using Fused Deposition Modeling (FDM), an extrusion-based AM technique. Despite the wide adoption of FDM, achieving optimal mechanical properties for functional applications remains challenging. To address this, multi-infill patterns incorporating alternating Gyroid and Cubic stacking sequences were explored to enhance performance metrics such as strength-to-weight ratio and failure resistance.

Polylactic Acid Plus (PLA+), a biodegradable material with improved toughness and heat resistance over standard PLA, was employed to fabricate specimens at a constant 60% infill density. Tensile evaluation was conducted in accordance with ASTM standard.

The results revealed the diverse mechanical responses across both single and multi-infill patterns, with significant variations in tensile strength and ductility depending on the geometry and stacking sequence. Within multi-infill configurations, the Gyroid-Cubic-Gyroid (GCG) pattern demonstrated a favorable balance of stiffness and ductility, while other configurations exhibited unique strengths influenced by their specific stacking sequences. Multi-infill designs were found to introduce distinct stress distribution characteristics due to their layered transitions, which provided opportunities for tailoring mechanical properties for specific applications.

This study underscores the potential of multi-infill strategies to

achieve customizable mechanical performance while offering insights into optimizing stacking sequences for tensile applications. The findings contribute to the development of sustainable additive manufacturing practices, with future research directed at improving interlayer bonding and exploring advanced hybrid geometries.

Index Terms- FDM, multi-infill patterns, tensile strength, PLA+, additive manufacturing

I. INTRODUCTION

The rapid advancement of 3D printing technologies, particularly Fused Deposition Modeling (FDM), has fundamentally transformed various industries, offering unprecedented possibilities in design, customization, and production efficiency. FDM, which involves the layer-by-layer deposition of thermoplastic materials, is widely adopted for both prototyping and the manufacturing of functional components due to its accessibility, cost-effectiveness, and versatility [1, 2]. Despite these advantages, FDM-printed parts, especially those fabricated from materials such as PLA+, are often limited by suboptimal mechanical properties, including lower strength, stiffness, and thermal stability compared to conventionally manufactured components. These limitations are exacerbated when producing parts with complex geometries or intricate internal features that are increasingly demanded in modern engineering applications. In response to these challenges, researchers and practitioners have explored the use of lattice structures—intricate networks of interconnected beams or struts—as a means to enhance the mechanical

properties of 3D-printed parts. Lattice structures offer a unique opportunity to achieve a balance between strength, weight efficiency, and material consumption. Specifically, multi-infill lattice structures, which combine different lattice patterns within a single part, provide an innovative solution for optimizing the mechanical behavior of FDM-printed components. By tailoring the internal structure of a part, it is possible to enhance various properties such as tensile strength, stiffness, and energy absorption, while reducing material usage and weight. Despite the theoretical advantages of multi-infill lattice structures, there is a noticeable gap in experimental studies that comprehensively assess their mechanical performance in real-world applications, particularly in the context of FDM and PLA+ materials. This paper aims to bridge this gap by investigating the tensile properties of multi-infill lattice structures, specifically focusing on how varying lattice patterns and infill configurations influence the performance of FDM-printed parts. Through a detailed experimental study, this research will compare the tensile performance of multi-infill lattice structures with traditional single-infill structures, providing valuable insights into the potential of multi-infill strategies for the optimization of FDM 3D-printed components. Ultimately, this study seeks to contribute to the development of advanced design methodologies that can enable the production of high-performance, lightweight components tailored to meet the demands of industries such as aerospace, automotive, and biomedical engineering.

II. LITERATURE REVIEW

Fused Deposition Modeling (FDM) is a widely accepted additive manufacturing (AM) technique due to its ability to shorten product development cycles and facilitate the fabrication of geometrically complex parts through layer-wise material deposition directly from CAD models, without requiring specialized tooling [1, 2]. The mechanical behavior of FDM-printed parts is influenced by numerous process parameters, which must be carefully optimized to enhance part strength, dimensional accuracy, and surface finish [3]. While FDM excels in design flexibility and prototyping, its

mechanical performance often lags behind that of injection-molded parts, necessitating targeted investigations into process parameter effects [4].

In order to explore the impacts of various process parameters on part characteristics, a fishbone diagram [5] presented shown in Figure 1, which visually maps out the interconnections between these parameters and their effects on different part properties. This diagram is derived from an aggregation of findings from several existing studies, illustrating how factors such as layer thickness, print speed, extrusion temperature, and infill density, among others, influence critical aspects like surface roughness, dimensional accuracy, tensile strength, and build time.

It is important to note that some process parameters demonstrate overlapping effects on multiple part characteristics. For instance, layer thickness and print speed directly influence both surface roughness and dimensional accuracy, while infill density has been found to impact tensile strength as well as the build time of parts. This indicates that optimization of a single parameter can lead to improvements in several part characteristics simultaneously. Additionally, parameters like multi-infill pattern and air gap have shown varying degrees of significance, highlighting the need for comprehensive optimization strategies that consider the interactions of multiple parameters.

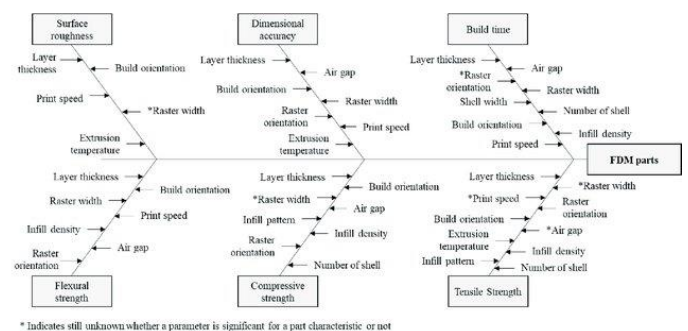


Figure 1: A fishbone diagram to illustrate the impacts of process parameters on part characteristics

Raster angle and build orientation significantly impact mechanical performance, surface roughness, and production cost. Gopi Mohan [6] showed that a 0° raster angle and horizontal build orientation optimize these metrics in ABS

specimens. Similarly, A. Nabavi-Kivi and Majid R. Ayatollahi [7] reported that a 0° raster angle combined with lower layer height enhances tensile strength, while tensile performance initially improves with increasing raster width before declining beyond a critical point.

Šibalić et al. [8] demonstrated that layer height critically affects inter-layer bonding strength, followed by deposition velocity. Qamar et al. [9] confirmed that smaller layer thicknesses and higher feed rates lead to improved tensile and flexural properties. Specimens printed in "on-edge" orientation exhibited the highest tensile strength, followed by flat orientation, with upright orientation showing the weakest performance.

Infill strategy is crucial for determining tensile strength, weight, and production efficiency. Giri et al. [3] found that rectilinear and concentric infill patterns yielded higher tensile strengths than Hilbert curve patterns. Yazar et al. [10] identified triangular infill patterns with 50% density as optimal for toughness and yield strength. Fernandez-Vicente et al [11] recommended honeycomb patterns for applications requiring high strength-to-weight ratios.

The microstructure of FDM-printed parts plays a pivotal role in their mechanical behavior. Rodriguez et al. [12] noted that voids and reduced molecular orientation during extrusion lower ABS sample strength compared to raw filaments. Enhancements such as inert gas printing, as explored by Thai li et al. [13], significantly improved mechanical properties in both ABS and nylon copolymers.

Wu et al. [14] found that PEEK outperformed ABS in tensile, compressive, and bending strength by over 100%, making it suitable for high-performance applications. Zaldivar [15] et al. reported that build orientation affected the thermal expansion coefficient of ULTEM samples, highlighting the interplay between thermal and mechanical properties in AM parts.

Process parameters such as air gap, infill density, print speed, and extrusion temperature critically influence mechanical properties. Lalegani et al. [16] emphasized that rectilinear infill patterns offer the best tensile strength, followed by honeycomb

and concentric arrangements. Dudescu et al. [17]. further highlighted the interplay between infill strategies and surface finish.

Research has consistently shown that higher infill densities improve tensile strength and stiffness but increase material costs and build times [18]. Pernet et al. [19] recommended honeycomb patterns for applications prioritizing strength-to-weight ratios, Shih et al. [20] showed that cold plasma treatment improves interlayer bonding strength in PLA, though prolonged treatment can degrade performance. Chemical treatments for surface texturing have also been explored, with mixed results regarding tensile strength [21].

Fiber reinforcement, ultrasonic strengthening, and damage/deformation studies have broadened the application scope of FDM [22]. For instance, Koziar et al. [23] successfully combined FDM and electrospinning to create mechanically stable filters with nanofibrous surfaces.

The majority of FDM studies focus on single infill patterns, leaving multi-infill strategies largely unexplored. Research by Dave et al. [24] and Lalegani Dezaki et al. [16] demonstrated that multi-infill pattern improves mechanical performance, especially in tensile applications. Multi-infill configurations, such as combinations of honeycomb and grid patterns, have shown superior strength-to-weight ratios compared to solid infills.

This research aims to fill the gap in understanding multi-infill strategies by systematically investigating their effects on the mechanical properties of FDM-printed parts. By comparing pure infill and multi-infill patterns, the study identifies configurations that optimize strength-to-weight ratios while minimizing material costs and production times.

Our study adopts a similar multi-infill strategy to investigate the effects of stacking sequences on tensile, compressive, and impact properties. Customized G-code was developed to fabricate PLA specimens with multi-infill configurations, and microscopic analysis of fractured surfaces was conducted to understand failure mechanisms.

III. RESEARCH METHODOLOGY

3.1 Materials and Printing Parameters

PLA+ was selected for its superior mechanical properties compared to standard PLA. It offers improved toughness, higher thermal resistance, and reduced brittleness, making it ideal for structural applications.

All test specimens were fabricated using a Creality Ender V3 SE FDM 3D printer. The specimens were printed in a flat orientation, with all layers aligned parallel to the XY plane. The thickness of the specimen corresponded to the Z-direction, while the longitudinal axis was aligned with the X-axis of the printer. A 1.75 mm diameter filament was extruded through a 0.4 mm nozzle, and custom toolpath files were created to accommodate the multi-infill patterns. These toolpath files were generated using Ultimaker Cura slicing software. The fixed printing parameters, including layer height, printing speed, and infill density, are detailed in Table 1 and shown in Figure 2.

Table 1: 3D printer Specifications

3D Printer parameters	Value
Max Printing Speed	250 mm/s
Printing Precision	0.1mm
Nozzle Diameter	0.4mm
Bed Temperature	≤ 100 °C
Max Nozzle Temperature	260° C
Machine Weight	6.5 kg
Size	365 x 345 x 458 mm
Bed Size	220 x 220 x 250 mm
Power Supply Input	Input AC 115V/230V Output DC 24V 270W



Figure 2: Creality Ender 3 V3 3D printer

The printing parameters, as shown in Table 2, were carefully optimized to ensure consistency and reproducibility across all test specimens.

Table 2: Sets of used process parameters

Description	Specification
Material	PLA+
Layer height (mm)	0.1
Wall line count	2
Top/Bottom thickness (mm)	0.2
Top/Bottom layer (mm)	0.2
Infill density	60%
Infill layer thickness (mm)	0.2
Bed temperature (°C)	70
Nozzle temperature (°C)	210
Printing speed (mm/s)	40
Retraction distance (mm)	5
Retraction speed (mm/s)	45

3.2 Infill Configurations

Seven distinct stacking sequences were designed to investigate the mechanical effects of multi-infill patterns as shown in Table 3. Each configuration combines Gyroid (G) and Cubic (C) patterns in various sequences to assess their tensile performance.

Table 3: Description of different stacking sequences

S. No	Stacking sequence	Designation	Description
1	S1	G	Entire specimen fabricated with Gyroid pattern
2	S2	CG	Specimen divided into two equal sections, one section fabricated with Gyroid and the other with Cubic pattern i.e. 50% Gyroid ,50%Cubic)
3	S3	GCG	Specimen divided into three equal sections, alternating between Gyroid and Cubic i.e. 33.33% Gyroid, 33.33% Cubic, 33.33% Gyroid
4	S4	CGC	Specimen divided into three equal sections, alternating between Cubic and Gyroid i.e. 33.33% Cubic, 33.33% Gyroid, 33.33% Cubic
5	S5	CGCGC	Specimen divided into five equal sections, starting and ending with Cubic (20% Cubic alternating with 20% Gyroid)
6	S6	GCGCG	Specimen divided into five equal sections, starting and ending with Gyroid (20% Gyroid alternating with 20% Cubic)
7	S7	C	Entire specimen fabricated with Cubic pattern

3.3 Testing

In this study, the tensile test specimens were designed using SolidWorks 2022 software in accordance with the specifications outlined in ASTM D638 standards [25] for tensile testing. The detailed geometry and dimensions of the specimens are illustrated in Figure 3, ensuring strict adherence to international testing protocols to maintain consistency and comparability of results. The same was printed twice for all stacking sequence to ensure dimensional accuracy as shown in Figure 4.

Uniaxial tensile testing was conducted to evaluate the tensile strength of the specimens using a Shimadzu Autograph UTM (Universal Testing Machine) with a load capacity of 100 kN. The tests were performed in accordance with the ASTM D638 [25], at a constant deformation speed of 5 mm/min until failure occurred. Testing was conducted under controlled room temperature conditions.

Stress-strain, load, and elongation data were recorded continuously using the machine's built-in software. Specimens were gripped in cross-wedge holders to ensure proper alignment and minimal slippage during testing. Figure 5 illustrates the Shimadzu Autograph UTM and setup of the tensile test and fractured specimen, showing a specimen mounted within the grippers.

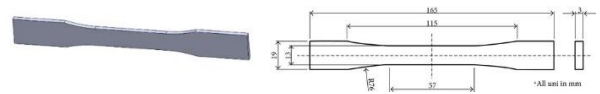


Figure 3: ASTM D638 Type I Tensile Specimen



Figure 4: 3D printed tensile specimen



Figure 5: Tensile test specimen design

IV. RESULTS AND DISCUSSION

The mechanical behavior of multi-infill specimens under quasi-static tensile loading was evaluated in accordance with ASTM D638 standards [25], with a focus on understanding the tensile properties of PLA+ components printed using various multi-infill stacking sequences. The experiments involved specimens with an infill density of 60%, covering pure Gyroid and Cubic configurations, along with various multi-infill stacking sequences, as shown in the stress-strain curves presented in Figure 6.

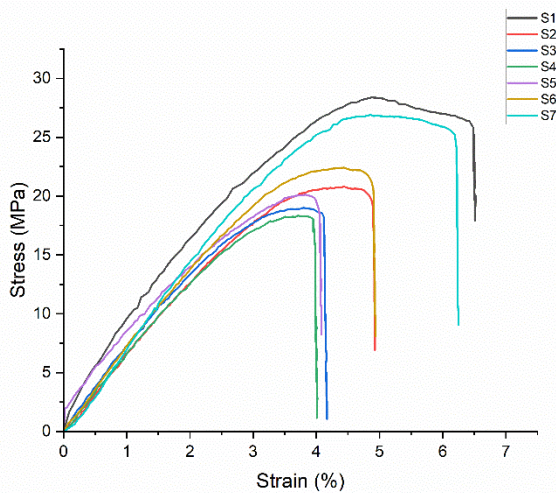


Figure 6: Stress strain plots of stacking sequences

Table 4: Mechanical behavior of all stacking sequences

S.No	Type of Stacking Sequence	Tensile Strength (MPa)	Strength to weight ratio (MPa/gram)	Young's modulus (GPa)
1	S1	28.37 ± 0.64	2.6	1.63 ± 0.03
2	S2	20.82 ± 0.44	1.90	1.23 ± 0.02
3	S3	18.99 ± 0.95	1.77	1.1 ± 0.05
4	S4	18.30 ± 0.56	1.67	1.05 ± 0.03
5	S5	20.12 ± 0.9	1.84	1.22 ± 0.05
6	S6	22.22 ± 1.2	2.03	1.36 ± 0.07
7	S7	26.78 ± 1.5	2.43	1.66 ± 0.06

Initially, all specimens exhibited an elastic response, marked by a linear relationship between stress and strain, as expected for typical FDM-printed materials. However, the transition to the plastic region occurred beyond the yield point, where permanent deformation became evident. This transition marked the onset of plasticity in the material, leading to a significant change in the specimen's mechanical response. The detailed mechanical properties of each configuration, including Young's modulus, tensile strength, and strength-to-weight ratio, are summarized in Table 4.

The S6 stacking sequence demonstrated the highest overall performance in terms of tensile properties, exhibiting a Young's modulus of 1.36 GPa, a tensile strength of 22.22 MPa, and a strength-to-weight ratio of 2.03 MPa/gram. These values were

notably superior to those observed in other multi-infill structures, highlighting the effectiveness of the S6 sequence for optimizing tensile strength and rigidity. The superior performance of S6 is attributed to its specific combination of material behavior, which optimally balances stiffness and ductility, as well as its ability to withstand higher loads.

In terms of mechanical response, the multi-infill structures displayed distinct bending-dominant and stretch-dominant behaviors, as classified by Pi, Y [26]. The S5 and S6 structures exhibited bending-dominant behavior, with significant moments acting at the junctions between walls. These moments caused the walls to bend, leading to a progressive deformation pattern characterized by lower stiffness and higher flexibility. Conversely, the S2 and S3 configurations demonstrated stretch-dominant behavior, where axial forces were supported by struts aligned with the loading direction, resulting in a more rigid structure with improved tensile performance.

The S6 configuration exhibited the highest maximum strain before failure, signifying extensive plastic deformation under tensile loading. The formation of plastic hinges at regions of maximum bending moments allowed localized deformation while facilitating further loading. This behavior was particularly apparent in the outer walls of the lattice structure, where initial failure was observed, followed by the propagation of failure towards the interior. The failure mode was characterized by a redistribution of stress within the remaining structure, causing sawtooth-like patterns in the stress-strain curves, which were more pronounced in the S3 configuration.

The failure mechanisms of bending-dominant and stretch-dominant structures under tensile loading were distinct. In stretch-dominant structures such as S3, compression occurred in the slanted walls, while tension was applied to the walls parallel to the loading direction. These structures exhibited a brittle failure mode with minimal deformation, marked by a sharp rupture at critical stress points. On the other hand, bending-dominant structures like S6 displayed a more ductile failure mode, where plastic hinges formed at the junctions of the walls, allowing for considerable deformation before

eventual fracture. The progressive failure in these structures resulted in greater overall ductility but reduced stiffness compared to stretch-dominant designs.

The experimental observations are consistent with previous studies conducted by Naik et al. and Sajjad [4, 26], who also identified the importance of stress concentrations at junction points and outer walls as initiators of failure. This progressive failure mode further emphasizes the strengths and limitations of bending-dominant versus stretch-dominant infill patterns in optimizing the tensile properties of FDM-printed components.

In terms of performance, configurations S1 and S7 showed predictable performance characteristics. The S1 configuration demonstrated higher isotropic strength, making it suitable for applications where uniform strength is required. In contrast, the S7 configuration exhibited superior stiffness, highlighting its potential use in applications where rigidity is the primary requirement. The multi-infill configurations, particularly S2 and S3, stood out due to their ability to combine the benefits of both Gyroid and Cubic patterns, offering a balanced performance in terms of both tensile strength and stiffness.

Among the multi-infill configurations, S2 achieved the highest tensile strength of 23.04 MPa and a strength-to-weight ratio of 2.23 MPa/gram. The improved performance of S2 is attributed to the alternating load distribution provided by the Gyroid layers and the increased stiffness contributed by the Cubic layers. This combination of infill strategies enhances both the load-bearing capacity and the structural efficiency of the components, making it a highly promising configuration for optimizing the tensile properties of PLA+ components in FDM printing.

V. CONCLUSION

This study demonstrates the effectiveness of multi-infill strategies in optimizing the tensile properties of FDM-printed PLA+ components. The experimental findings highlight that multi-infill configurations significantly influence mechanical behavior, particularly in terms of tensile strength, stiffness, and

ductility. Key takeaways from the study include:

- **Superior Tensile Performance:** Multi-infill configurations, particularly S2 (Gyroid-Cubic) and S6 (Gyroid-Cubic-Gyroid), exhibited enhanced tensile strength and strength-to-weight ratios, outperforming single-infill structures.
- **Synergistic Effect of Infill Patterns:** The integration of Gyroid and Cubic infills provided a balanced mechanical response, where Gyroid layers contributed to isotropic strength and ductility, while Cubic layers improved stiffness.
- **Failure Mechanisms:** The study revealed distinct failure behaviors, with bending-dominant structures offering improved ductility and energy absorption, whereas stretch-dominant structures exhibited higher rigidity but brittle failure characteristics.
- **Design Optimization for FDM Applications:** The insights gained from this research can inform the selection of infill strategies for load-bearing applications, offering a pathway to enhanced mechanical performance while maintaining material efficiency.

Future work should explore additional multi-infill configurations, investigate their fatigue resistance, and optimize interlayer bonding strategies to further improve the structural integrity of FDM-printed components. The results contribute to advancing additive manufacturing methodologies, making them more viable for engineering applications requiring high-performance, lightweight structures.

ACKNOWLEDGMENT

I am profoundly thankful to my friends for their unwavering support throughout this research, as well as my peers at the UET Peshawar and PCSIR Labs Complex Peshawar whose assistance and collaboration were vital during this journey.

REFERENCES

1. Kumaresan, R., et al., *Fused deposition modeling: process, materials, parameters, properties, and applications*. The International Journal of Advanced Manufacturing Technology, 2022. **120**.

2. Kristiawan, R.B., et al., *A review on the fused deposition modeling (FDM) 3D printing: Filament processing, materials, and printing parameters*. Open Engineering, 2021. **11**(1): p. 639-649.
3. Giri, J., et al., *Effect of process parameters on mechanical properties of 3d printed samples using FDM process*. Materials Today: Proceedings, 2021. **47**: p. 5856-5861.
4. Naik, M., D.G. Thakur, and S. Chandel, *An insight into the effect of printing orientation on tensile strength of multi-infill pattern 3D printed specimen: Experimental study*. Materials Today: Proceedings, 2022. **62**: p. 7391-7395.
5. Dey, A. and N. Yodo, *A Systematic Survey of FDM Process Parameter Optimization and Their Influence on Part Characteristics*. Journal of Manufacturing and Materials Processing, 2019. **3**: p. 64.
6. Gopi Mohan, R., et al., *Comparitive analysis of mechanical properties of FDM printed parts based on raster angles*. Materials Today: Proceedings, 2021. **47**: p. 4730-4734.
7. Nabavi-Kivi, A., M.R. Ayatollahi, and N. Razavi, *Investigating the effect of raster orientation on fracture behavior of 3D-printed ABS specimens under tension-tear loading*. European Journal of Mechanics - A/Solids, 2023. **99**: p. 104944.
8. Šibalić, M., A. Vujović, and J. Šaković Jovanović, *Unconventional use of FDM printing method for testing the delamination of PVA material for different layer height*. Procedia Structural Integrity, 2024. **56**: p. 78-81.
9. Qamar Tanveer, M., et al., *Effect of infill pattern and infill density on mechanical behaviour of FDM 3D printed Parts- a current review*. Materials Today: Proceedings, 2022. **62**: p. 100-108.
10. Yazar, A., et al., *Effect of Infill Density and Infill Pattern on Mechanical Properties in Fused Deposition Modeling (FDM)*. 2021.
11. Fernandez-vicente, M., et al., *Effect of Infill Parameters on Tensile Mechanical Behavior in Desktop 3D Printing*. 3D Printing and Additive Manufacturing, 2016. **3**: p. 183-192.
12. Mishra, P., et al., *Microstructural characterization and mechanical properties of additively manufactured 21-6-9 stainless steel for aerospace applications*. Journal of Materials Research and Technology, 2023. **25**: p. 1483-1494.
13. Le, T.-H., et al. *Microstructure Evaluation and Thermal-Mechanical Properties of ABS Matrix Composite Filament Reinforced with Multi-Walled Carbon Nanotubes by a Single Screw Extruder for FDM 3D Printing*. Applied Sciences, 2021. **11**, DOI: 10.3390/app11198798.
14. Wu, W., et al. *Influence of Layer Thickness and Raster Angle on the Mechanical Properties of 3D-Printed PEEK and a Comparative Mechanical Study between PEEK and ABS*. Materials, 2015. **8**, 5834-5846 DOI: 10.3390/ma8095271.
15. Zaldivar, R.J., et al., *Influence of processing and orientation print effects on the mechanical and thermal behavior of 3D-Printed ULTEM® 9085 Material*. Additive Manufacturing, 2017. **13**: p. 71-80.
16. Lalegani Dezaki, M. and M.K. Mohd Ariffin *The Effects of Combined Infill Patterns on Mechanical Properties in FDM Process*. Polymers, 2020. **12**, DOI: 10.3390/polym12122792.
17. Dudescu, M.C., L. Racz, and F. Popa, *Effect of infill pattern on fatigue characteristics of 3D printed polymers*. Materials Today: Proceedings, 2023. **78**: p. 263-269.
18. Nomani, J., et al., *Effect of layer thickness and cross-section geometry on the tensile and compression properties of 3D printed ABS*. Materials Today Communications, 2020. **22**: p. 100626.
19. Pernet, B., J. Nagel, and H. Zhang, *Compressive Strength Assessment of 3D Printing Infill Patterns*. Procedia CIRP, 2022. **105**: p. 682-687.
20. Shih, C.-C., et al., *Effects of Cold Plasma Treatment on Interlayer Bonding Strength in FFF Process*. Additive Manufacturing, 2018. **25**.
21. Hiremath, S., et al., *Exploring the impact of epoxy coated 3D-Printed polymers on surface roughness and mechanical behavior: An experimental and numerical study*. Results in Engineering, 2024. **23**: p. 102779.
22. Memarzadeh, A., et al., *Advancements in additive manufacturing of polymer matrix composites: A systematic review of techniques and properties*. Materials Today

Communications, 2023. **36**: p. 106449.

23. Kozior, T., et al., *Electrospinning on 3D Printed Polymers for Mechanically Stabilized Filter Composites*. Polymers, 2019. **11**: p. 2034.

24. Dave, H., et al., *Effect of multi-infill patterns on tensile behavior of FDM printed parts*. Journal of the Brazilian Society of Mechanical Sciences and Engineering, 2021. **43**.

25. International, A., *Standard Test Method for Tensile*

Properties of Plastics. ASTM International: West Conshohocken, PA.

26. Pi, Y., et al., *Crack propagation and failure mechanism of 3D printing engineered cementitious composites (3DP-ECC) under bending loads*. Construction and Building Materials, 2023. **408**: p. 133809.

AUTHORS

First Author – Noor Faraz Khan, Department of Mechanical Engineering, University of Engineering & Technology (UET), Peshawar.

Second Author – Dr. Abdul Shakoor, Department of Mechanical Engineering, University of Engineering & Technology (UET), Peshawar.

Third Author – Muhammad Bilal Afzal, Pakistan Council of Scientific and Industrial Research (PCSIR).

Fourth Author – Atif Shehzad, NED University of Engineering & Technology

Fifth Author – Fazli Subhan, Pakistan Council of Scientific and Industrial Research (PCSIR)

Sixth Author – Kamran Ahmed, Sui Northern Gas Pipelines Limited

Correspondence Author – Noor Faraz Khan,